

Metallic ions drift in hybrid bonding integration modeling, towards the evolution of failure criterion

MANZANAREZ Hervé

MOREAU Stéphane

CUETO Olga

Univ. Grenoble Alpes, CEA, LETI, F-38000 Grenoble France.
stephane-nico.moreau@cea.fr

Abstract—Copper ions drift is modeled in the case of hybrid bonding integration. The continuity equation is coupled to the Poisson’s equation and a copper ion concentration saturation is assumed. A 1D geometry simulation is initially realized to validate the model and 2D geometry simulations of hybrid bonding are analyzed by looking the time to percolate (TTP).

Index Terms—Hybrid bonding, copper ions drift, failure criterion, time to percolate.

I. INTRODUCTION

The continuous race to higher performance and compactness has led to the introduction of 3D integration in CMOS ICs. Among the different schemes to obtain 3D devices, the last decade has shown that direct bonding and more recently hybrid bonding (HB) was a key enabler for 3D high density integration [1]. Roughly, it consists in putting into contact two surfaces (wafer-to-wafer or die-to-wafer) to create interconnects by direct bonding (Fig. 1). This process requires to solve technological challenges, in particular a high level of cleanliness interface, an ultra smooth surface, and an ultra-precise alignment accuracy between the two surfaces. The misalignment cause copper to be directly in contact with the surrounding dielectric material. This could lead to reliability issues, dielectric breakdown [2]–[4] mainly, and must be investigated to evaluate the risk level.

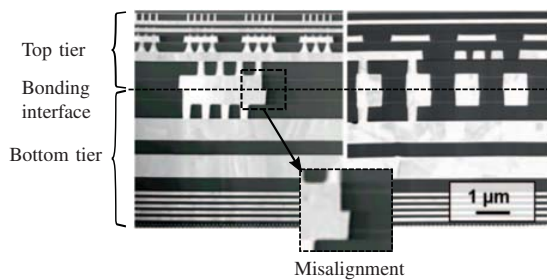


Fig. 1. TEM cross sections of 3D stacked image sensors with 8.8 (left) and 1.44 μm -pitch (right) [1]. Dashed box illustrates the top/bottom misalignment.

This paper aims at investigating the copper diffusion/drift phenomena in the context of HB technology by means of numerical approach. The “reference” diffusion/drift model provides good results for time dependant dielectric breakdown (TDDB) in 1D condition [5]. However, the HB geometry

This work was funded thanks to the French National programme “Programme d’Investissement d’Avenir IRT Nanoelec” ANR-10-AIRT-05.

intrinsically requires a 2D or 3D representation and the “reference” model fails to take into account the concentration variation due to the complexity of the boundary conditions. Consequently, a second model is proposed to overcome this problem. Both models are compared and the influence of voltage, temperature, misalignment, saturation concentration and failure criteria is presented and discussed.

II. MODELS

The time evolution of the copper ions concentration C is described by the usual variational principle of the continuity equation coupled with the Poisson’s equation for electrostatics:

$$\frac{\partial C}{\partial t} = \nabla \cdot (\Lambda \nabla \mu) \quad (1)$$

$$\nabla \cdot (\epsilon_r \epsilon_0 \nabla V) = -qC \quad (2)$$

where the electrochemical potential μ and the mobility Λ can be described in terms of derivatives of Gibbs free energy [6]:

$$\mu = \frac{\partial G}{\partial C} + qV \quad \text{and} \quad \Lambda = D \left(\frac{\partial^2 G}{\partial C^2} \right)^{-1}$$

In a first approach, the diffusion coefficient D is assumed to be independent of the copper ions concentration $D = D_0 \exp(-\beta E_a)$ with $\beta = 1/k_B T$ and E_a is the activation energy.

The dimensionless forms of the equations (1) and (2) are obtained by defining the scaling parameters $t_0 = L_0^2/D$ and $V_0 = (\beta q)^{-1}$:

$$\frac{d\phi}{dt} = \tilde{\nabla} \cdot \left[\tilde{\nabla} \phi + \left(\frac{\partial^2 G}{\partial \phi^2} \right)^{-1} \tilde{\nabla} \tilde{V} \right] \quad (3)$$

$$\tilde{\nabla}^2 \tilde{V} = -\Gamma \phi; \quad \Gamma = \frac{\beta C_0 (qL_0)^2}{\epsilon_r \epsilon_0} \quad (4)$$

where $\phi = C/C_0$, $\tilde{V} = V/V_0$, $\tilde{\nabla} = L_0 \nabla$ and Γ are dimensionless quantities.

Some studies [5], [7], [8] assume an approximation of the Gibbs free energy such as:

$$G = \frac{C_0}{\beta} \phi \ln \phi + \Delta H \quad (5)$$

Equation (5) is a good approximation for low ions copper concentration value, in other words $\phi \ll 1$.

The second derivative Gibbs free energy:

$$\frac{\partial^2 G_1}{\partial \phi^2} = \frac{1}{\phi} \left(1 + \beta \phi \frac{\partial^2 \Delta H}{\partial \phi^2} \right) \approx \frac{1}{\phi} \quad (6)$$

In this work, a second model is introduced. We assume that the copper ions Cu^{2+} drift is done via a number of limited free sites available in the dielectric material. In these conditions, the divergence concentration at the cathode is not possible and a solution is found by the assumption that an equilibrium concentration saturation occurs at $C = C_0$, which results in the modification of the following Gibbs free energy like:

$$G = \frac{C_0}{\beta} [\phi \ln \phi + (1 - \phi) \ln (1 - \phi)] + \Delta H \quad (7)$$

This condition can be imposed easily with the thermodynamical condition to the second derivative Gibbs free energy of mixing:

$$\frac{\partial^2 G_2}{\partial \phi^2} = \frac{1}{\phi(1 - \phi)} \left[1 + \beta \phi(1 - \phi) \frac{\partial^2 \Delta H}{\partial \phi^2} \right] \approx \frac{1}{\phi(1 - \phi)} \quad (8)$$

Such an approach allows to stop the contribution of the electric potential on the concentration evolution when the saturation equilibrium is obtained. Both models (equations (6) and (8)) postulate that the entropy contribution is greater than the enthalpy contribution ΔH .

This paper will initially present a comparison of the “reference” model (equation (3), (4) and (6)) and our “saturation” model (equation (3), (4) and (8)) in one dimension under the boundary conditions shown in Fig. 2. The scaling geometric parameter is taken to be equal to the dielectric domain length $L_0 = L$.

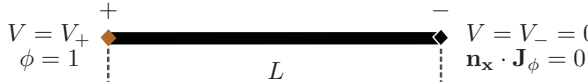


Fig. 2. 1D model for metal ions diffusion/drift study (dielectric illustrated only); boundary conditions.

Secondly, a 2D structure is used to investigate the HB technology from the diffusion/drift point of view (Fig. 3). Misalignment induces a source term of copper ions in the dielectric media (Fig. 3.a2) for both anode and cathode boundaries. Parameters used are listed in TABLE I.

TABLE I
PHYSICAL AND DESIGN PARAMETERS

Description	Symbol [unit]	Value
Electric potential	V_+ [V]	0 - 30
Homogeneous temperature	T [°C]	100 - 350
Saturation concentration	C_0 [$at.m^{-3}$]	10^{23} - 10^{26}
Dielectric domain length	L [nm]	200 and 600*
Misalignment *	L_{shift}^* [nm]	20* - 150*
Energy activation	E_a [eV]	0.653
Pre-exponential factor	D_0 [$m^2.s^{-1}$]	$1.68.10^{-14}$
Dielectric constant	ϵ_r	3.9
Dielectric breakdown	E_{bd} [$V.m^{-1}$]	10^8

*only in 2D

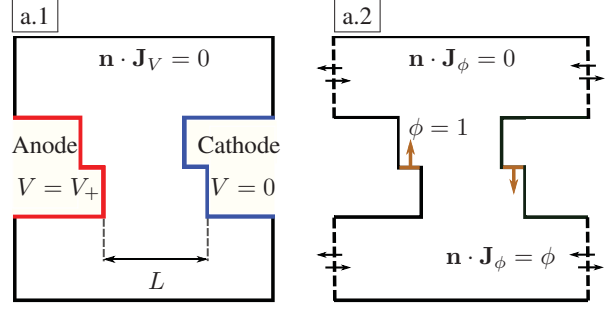


Fig. 3. 2D model for hybrid bonding-based interconnect (dielectric illustrated only), (a.1) electric potential boundary conditions, and (a.2) copper ions concentration boundary conditions.

III. SIMULATION RESULTS AND DISCUSSION

A. “Reference” model vs. “saturation” model: a 1D geometry

COMSOL Multiphysics® is used to solve the previous dimensionless set of equations. Fig. 4 shows the time evolution of the ions concentration profile and the electrical potential V for the 1D geometry (Fig. 2). The “reference” model results (Fig. 4.a.1) shows a divergence of the concentration at the cathode ($x=L$). This divergence induced a strong electric potential variation localised mainly at the cathode [9]. Achanta et al. [9] defined the time to failure (TTF) as the instance in time when the electric field at the cathode exceeds the breakdown strength. First, we have chosen this criterion to compare our model to the “reference” one.

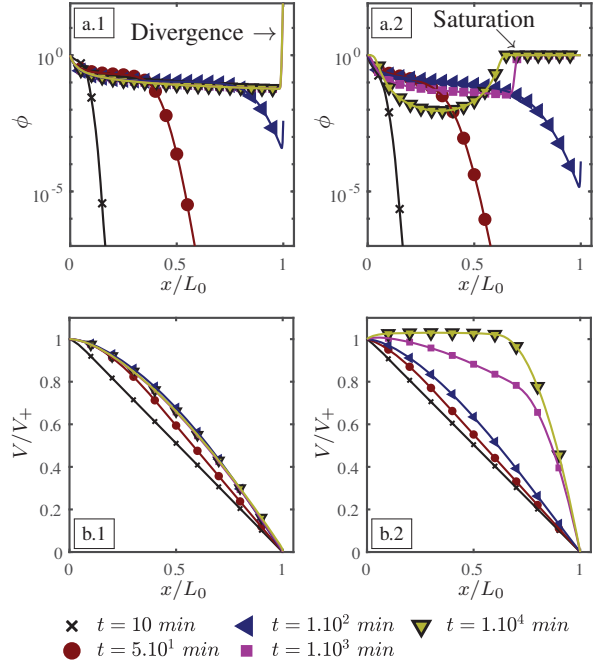


Fig. 4. ϕ vs. $\frac{x}{L_0}$ (a.1 and a.2) and $\frac{V}{V_+}$ vs. $\frac{x}{L_0}$ (b.1 and b.2) for different times in 1D geometry. The results of the “reference” model and the “saturation” model are respectively represented by the couple of plots (a.1, b.1) and (a.2, b.2). $C_0 = 10^{24} at.m^{-3}$, $V_+ = 20 V$.

Our model (Fig. 4.a.2) induces the accumulation of copper ions in free sites until a maximum saturation value is reached.

Due to the saturation mechanism, an electric potential variation inside the dielectric domain can lead, near the cathode, to electric field values larger than the dielectric strength. In addition, for long periods ($t > 10^4 s$) the maximum of the electric potential slightly exceeds the maximum initial value imposed on the anode, and this for a wide spatial area ($0 < x < 0.6$). This electric potential field significantly deforms the near-cathode field.

The influence of C_0 is shown in Fig. 5. While the dielectric breakdown value is reached in all cases for the “reference” model (Fig. 5.a.), our model shows that there is a saturation concentration limit value for the internal electric field to exceed the failure criterion (Fig. 5.b.). When the concentration saturation value is less than $5.10^{24} at.m^{-3}$, the copper ions drift does not modify the electric field sufficiently to induce a dielectric breakdown (*i.e.* $E < E_{bd}$). Thus, the estimation of this concentration becomes a crucial issue.

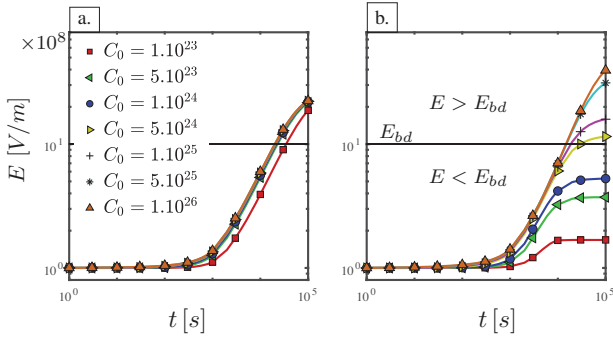


Fig. 5. E vs. t for different concentration saturation C_0 . The results of the “reference” model and the “saturation” model are respectively represented by the plot (a.) and (b.).

B. “Saturation” model and hybrid bonding-based geometry

Currently, wafer-to-wafer HB technology provides interconnect pitches in the range of 1 to $10 \mu m$ and an average misalignment between tiers of $200 nm$ [1], [10]. Pitch shrinkage requires by future applications potentially increases reliability issues. In that context, this study focused on extreme case with a pitch of $1.2 \mu m$, which corresponds to a typical dielectric domain length between the anode and the cathode of $0.6 \mu m$. The saturation concentration limit was set to $C_0 = 10^{26} at.m^{-3}$ to calibrate our model with previous studies [11].

Fig. 6 shows the copper ions concentration evolution only produced by the thermal diffusion mechanism. In order to understand the internal electric field induced by the presence of copper ions, two cases were compared: the diffusion equation (3) is solved (i) without coupling with the Poisson’s equation $\nabla \cdot \tilde{V} = 0 \forall t$ (usual Fick law) (Fig. 6.a.1-3), or (ii) by coupling with the Poisson’s equation but the anode electric potential is fixed to zero (Fig. 6.b.1-3).

For the first case (i), the two source terms create two areas that grow symmetrically until they gradually merge in the middle of the longer path between the anode and the cathode.

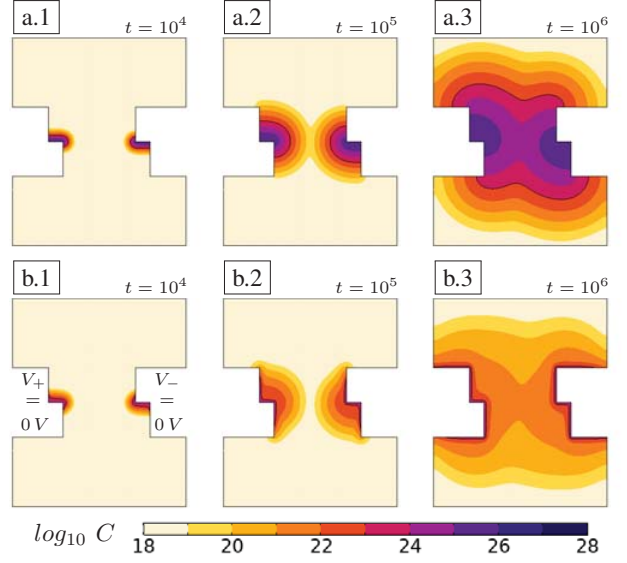


Fig. 6. 2D model for hybrid bonding-based interconnect with the “saturation” model: a- copper ions concentration evolution without electric physics, b- copper ions concentration evolution with electric physics and the anode electric potential $V = 0 V$.

For the second case (ii), the inclusion of ionized particles creates an internal electric field that opposes to the conventional thermal diffusion. When the copper ions concentration is very low ($\phi \ll 1$), the electric driving force is weaker than the thermal diffusion driving force ($\nabla \tilde{V} \ll \nabla \phi$). However, when the copper ions concentration is very high ($\phi \approx 1$), the electric driving force is stronger than thermal diffusion driving force ($\nabla \tilde{V} \gg \nabla \phi$) changing significantly the diffusion mechanism. Thus, the internal electric field induced by the copper ions inclusion under the dielectric material seems to act as a diffusion barrier for high concentrations.

Fig. 7 shows the effect of the external electric field on the diffusion dynamics. As can be seen, the presence of an external electric field breaks the symmetry between the two copper ions sources. If we only look at the diffusion along the x-axis, the copper ions displacement is accelerated in the direction of the cathode. This implies that the ions from the anode will penetrate more quickly in the dielectric medium and in greater number. At the opposite, the ions from the cathode will be more easily prevented to penetrate the dielectric region.

Furthermore, the intensity of the external electric field changes the topology of copper ions concentration between anode and cathode. As an example, in Fig. 7a.1-3, a copper ions concentration evolves until there is a connection between anode and cathode (percolation mechanism) for a threshold value of $C_{th} = 10^{21} at.m^{-3}$ (light orange/deep orange on log scale of Fig. 7) at $t = 10^6 s$ (arbitrary time). For $C_{th} = 10^{22} at.m^{-3}$, the domains never connect. In Fig. 7b.1-3, the connected space for $C_{th} = 10^{21} at.m^{-3}$ appears earlier ($t = 10^5 s$) and there is no connected space for $C_{th} = 10^{22} at.m^{-3}$. Finally, when the anode electric potential is sufficiently high, a connected space

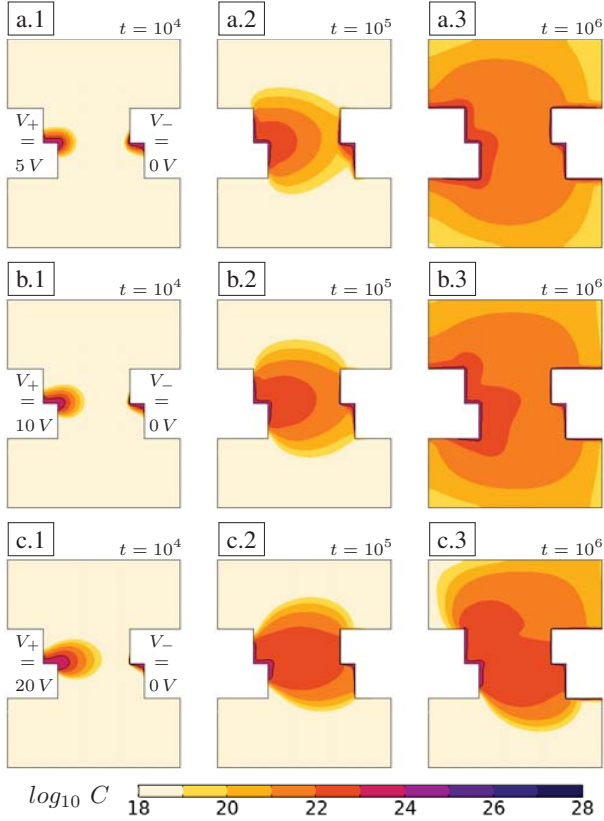


Fig. 7. Effect of the external electric potential for different times t [s] and different electric potential: a- $V_+ = 5$ V; b- $V_+ = 10$ V and c- $V_+ = 20$ V.

for $C_{th} = 10^{22} \text{ at.m}^{-3}$ exists (Fig. 7.c.3).

Regarding the standard TTF estimation, a direct calculation of the electric field at the cathode is inappropriate because peak effect occurs with consequently mesh-dependance. Hwang et al. [12] defined the TTF as the time at which the copper ions concentration at the cathode is 0.1% of the solubility (saturation concentration in our case). Although interesting this failure criterion is not satisfactory in our case because of the term source at the cathode. Finally, we defined the percolation time when, for a chosen copper ions concentration value, a topological connected space exists between anode and cathode. A range of values between 10^{20} and $10^{24} \text{ at.m}^{-3}$ is analysed at each time step and a time to percolate (TTP) is extracted when a connection is encountered.

Fig. 8 shows the TTP for different external electric potentials (8.a) and different misalignments (8.b). As it was seen in previous studies in 1D [12], the TTP seems to follow exponential laws:

$$t_{TTP}(V) \propto \exp(\alpha_1 V_+)$$

$$t_{TTP}(L_{shift}) \propto \exp(\alpha_2 L_{shift})$$

where $\alpha_1 \approx -0.6 \text{ V}^{-1}$ and $\alpha_2 \approx -5.10^6 \text{ m}^{-1}$. To the extent that misalignment is an experimental stochastic variable

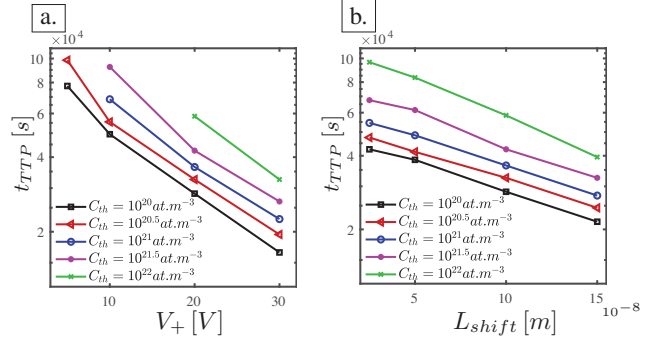


Fig. 8. TTP variation for different conditions: a- electric potential V_+ ranging from 5 to 30 V for a misalignment value $L_{shift} = 100 \text{ nm}$; b- misalignment L_{shift} ranging from 25 to 150 nm for $V_+ = 20$ V.

ranging from 0 to 200 nm [1], the dependence of the TTP on misalignment cannot be overlooked.

IV. CONCLUSIONS AND PERSPECTIVES

To the best of our knowledge, this paper presents the first model to investigate copper ions diffusion/drift in dielectric for hybrid bonding-based IC. This model introduces a copper concentration saturation mechanism that modifies the electrical field until the dielectric breakdown. A new failure criterion, time to percolate, is defined to overcome limitations of current ones dedicate to 1D geometry. In a near future, the TTP must be linked to the TTF using experiments and more complete topological analysis, in particular on the variation of the electric field.

REFERENCES

- [1] J. Jourdon et al., in *2018 IEEE International Electron Devices Meeting (IEDM)*, Dec 2018, pp. 7.3.1–7.3.4. <https://doi.org/10.1109/IEDM.2018.8614570>
- [2] J. P. Borja et al., *Dielectric Breakdown in Gigascale Electronics: Time Dependent Failure Mechanisms*. Cham: Springer International Publishing, 2016, ch. General Theories, pp. 11–19.
- [3] J. W. McPherson, *Microelectronics Reliability*, vol. 52, no. 9, pp. 1753–1760, 2012. [Online]. Available: <https://doi.org/10.1016/j.microrel.2012.06.007>.
- [4] T. K. S. Wong, *Materials*, vol. 5, pp. 1602–1625, 2012. <https://doi.org/10.3390/ma5091602>
- [5] R. S. Achanta et al., *Journal of Applied Physics*, vol. 103, no. 1, p. 014907, 2008. <https://doi.org/10.1063/1.2828048>
- [6] N. Pottier, *Physique statistique hors d'équilibre*. EDP Sciences, 2007, ch. 2, p. 42.
- [7] J. D. McBrayer et al., *J. Electrochem. Soc.*, vol. 133, no. 6, pp. 1242–1246, 2002. <https://doi.org/10.1149/1.2108827>
- [8] K.-S. Kim et al., *Jpn. J. Appl. Phys.*, vol. 41, no. L99, pp. L99–L101, 2002. <https://doi.org/10.1143/JJAP.41.L99>
- [9] R. S. Achanta et al., *Applied Physics Letters*, vol. 91, no. 23, p. 234106, 2007. <https://doi.org/10.1063/1.2823576>
- [10] E. Beyne et al., *2017 IEEE International Electron Devices Meeting (IEDM)*, pp. 32.4.1–32.4.4, 2017. <https://doi.org/10.1109/IEDM.2017.8268486>
- [11] J. L. Plawsky et al., *Journal of Materials Science: Materials in Electronics*, vol. 23, no. 1, pp. 48–55, Jan 2012. <https://doi.org/10.1007/s10854-011-0406-x>
- [12] S.-S. Hwang et al., *Journal of Applied Physics*, vol. 101, no. 7, p. 074501, 2007. <https://doi.org/10.1063/1.2714668>